Learning-Based Endovascular Navigation Through the Use of Non-Rigid Registration for Collaborative Robotic Catheterization

Wenqiang Chi[1], Jindong Liu[1], Hedyeh Rafii-Tari[1], Celia Riga[2], Colin Bicknell[2] and Guang-Zhong Yang[1], *Fellow*, *IEEE*

***Abstract*— This paper improves a semi-automatic robotic catheterization platform based on previous works [9] by proposing a method to address subject variability. It incorporates anatomical information in the process of catheter trajectories optimization, hence can adapt to the scale and orientation differences among subjects. Statistical modeling is implemented to encode the catheter motions of both proximal and distal sites from demonstrations of one vascular model. Non-rigid registration is applied to find a warping function to map catheter tip trajectories onto other anatomically-similar but shape/scale/orientation different models. Such function can finally generate a robot trajectory to conduct a collaborative catheratization task. Experiments investigate the proposed method in different vascular phantoms. The success rate for semi-automatic cannulation is high, which suggest the method can be potentially applied to different endovascular tasks and vasculature. The proposed robotic approach also show significant improvements in the quality of catheterization over manual approach by achieving smoother and safer catheter paths and reducing contact forces. This work provides insights into catheter task planning and an improved design of hands-on, ergonomic catheter navigation robots.**

I. INTRODUCTION

Endovascular intervention has become a promising treatment to vascular diseases, for that catheters and guidewires are navigated by the clinician to reach the target vasculature. In recent years, there has been a growing interest in robot-assisted catheter navigation systems. Compared to manual catheterization, these platforms could provide advantages such as added stability and precision of motion, increased comfort for the operator, and reduced radiation from the ionizing sources [1]. However, most existing platforms have been designed without consideration of natural bedside manipulation skills and many master controllers fail to utilize the operator's experience obtained from conventional catheterization. Recent advances in both imaging and robotic technologies could provide the possibility for an enhanced robot-assisted catheterization. Learning the essential interactive behavior patterns between the catheter and blood vessels as well as between the operator and the catheter from demonstrations, incorporating anatomical information from pre-operative images, and applying them to a semi-autonomous and collaborative robotic catheterization within different anatomical geometries, can reduce the cognitive workload of the operator while improving the quality of the catheter insertion.

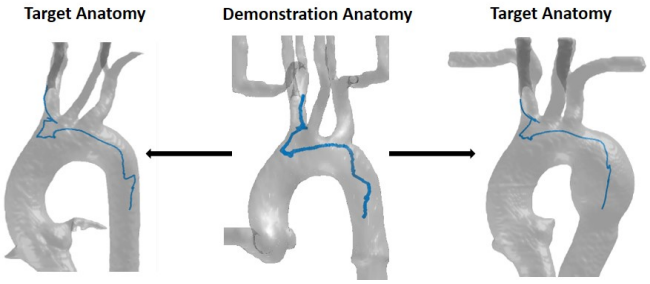

Fig. 1. Examples of catheter tip motion (blue line) transformation from a demonstration anatomy (center) to target anatomies (left and right)

One of the main commercially available steerable platforms for endovascular intervention is the Magellan System (Hansen Medical, Mountain View, CA, USA), while many master/slave platforms have also been developed for standard catheters in the research domain [2]. However, in most existing solutions, instrument manipulation is achieved through multi-DOF haptic interfaces or joysticks which alter the natural patterns of catheter manipulation. Therefore, there has been a growing interest in developing ergonomic master interfaces that can potentially utilize the experience-related skills of the endovascular interventionalist [3].

Recent research explores the application of the "learning from demonstration" framework, commonly used in robotics, towards automating whole or part of the procedure in minimally invasive surgery applications. These studies include complete automation of time-consuming and repetitive tasks [5], as well as collaborative surgery in which the control is shared back and forth between the operator and the robot [6]. Recent studies have looked into generalizing learned demonstrations to previously unseen initial conditions [7], as well as an adaptive trajectory planning to deal with dynamic changes in the environment [8]. In the field of endovascular intervention these learning-based techniques have been used for automation of motion trajectories from expert demonstrations for the same catheterization task, by a robotic driver, demonstrating potential improvements over manual catheterization [9]. The pre-operative images for surgical navigation also offer the possibility for robotic path planning based on anatomical information. Commercial robotic system such as the Sensei X system (Hansen Medical, Mountain View, CA, USA) integrated 3D electroanatomic mapping (EAM) technology for improved navigation of the robotic

[1]Wenqiang Chi, Jindong Liu, Hedyeh Rafii-Tari and Guang-Zhong Yang are with the Hamlyn Centre for Robotic Surgery, Imperial College London, SW7 2AZ, London, UK (email:wenqiang.chi10@imperial.ac.uk)

[2]Celia Riga and Colin Bicknell are with Department of Surgery and Cancer, Imperial College London, St Marys Hospital, W2 1NY, London, UK

catheter [10]. Other research has studied skeletonization techniques, extracted from CT angiography (CTA), for extracting blood vessel centerlines towards efficient path planning for endovascular surgical tools [11]. More recently, a cooperative robotic catheterization platform was developed for adapting learned trajectories to different vascular anatomies using shared-control navigation [12]. However, these frameworks did not consider image-based anatomical information, and as such did not incorporate difference in task scale and orientation. The use of anatomical landmarks to aid semi-autonomous robotic catheterization within different anatomical settings has not been explored as yet.

Based on our previous work [9], this paper improves the semi-automatic robotic catheterization by addressing the subject-specific variability, through incorporating the anatomical information obtained from pre-operative image data. In the proposed approach, catheter tip positions at the distal end as well as axial/rotational motions exerted by the operator at the proximal end were obtained from the demonstration on vascular models. They are jointly used to train statistical models that encodes the essential motion patterns of the operator and the catheter motions, together with the model's anatomical information, a trajectory generator is proposed to generated patient-specific trajectories that can potentially tolerate catheterization task scale and orientation difference. Such trajectory generator can generate a robotic catheter control sequence for different vascular models by integrating the latter's anatomical information through non-rigid registration techniques. The approach is verified by testing the generated robotic trajectories onto different vascular models, achieving a high success rate for cannulation tasks. The quality of the catheterization is further assessed by comparing the proposed robotic approach against manual techniques. The robotic approach achieved smoother and safer catheter paths that potentially associated with reduced risks in perforation, dissection and stroke. The proposed platform provides insights into endovascular task planning based on pre-operative image data, and a hands-on catheter navigation system that utilized the natural skills of the operator. Fig. 1 demonstrates the idea of our approach for mapping catheter tip motions in different anatomies.

II. Materials and Methods

An overview of the proposed methods for adapting robotic trajectories into anatomical variability is shown in Fig. 2. The details is explained in this section including the methodologies for catheter motion modeling, transformation of the catheter tip motion and trajectory optimization. The validation method for each module is introduced as well.

A. Catheterization Motion Modeling

Our method for catheterization motion modeling is based on the previous work of the authors in [9]. The Gaussian Mixture Models (GMM) was used to train models of catheter proximal motions and catheter tip motions jointly from demonstrations. The objectives are 1) capture the underlying motion patterns of the catheter for a specific catheterization task in a specific type of aortic arch (Type I); 2) encode the correlation between catheter proximal motions and tip motions; and 3) produce smoothed robotic trajectories that were executed on the robotic catheterization platform [9].

Task Demonstration: Catheter proximal motion data and tip motion data were collected from an expert vascular surgeon (having performed over 300 endovascular procedures). The specific catheterization task was cannulation of the innominate artery of a silicone-based, transparent, anthropomorphic phantoms, of a standard type I aortic arch. Three Type I arch models were used in this study, including a healthy arch (Phantom A) (Fig. 3(b)), one with an aneurysm (Phantom B) (Fig. 3(c)) and one with a re-created stenosis (Phantom C) (Fig. 3(d)) (Elastrat Sarl, Switzerland). Six demonstrations were collected from each phantom. The demonstrations from one phantom were used to train the trajectory generator while those from other two phantoms were taken to verify the performance of the robot trajectory. The starting/ending positions of the catheter tip were specified as the level in parallel to the origin of the left coronary artery, and the bifurcation site of the right common carotid artery and the right subclavian artery, respectively. A 5F shaped catheter and a 0.035" guidewire were used in this study. A camera was mounted above the vascular phantom, 2D projected images of the phantom was then displayed on a monitor for navigation. Catheter tip positions (x,y,z) were collected from a six DoF electromagnetic (EM) position sensor (Aurora, NDI) which was attached to the catheter tip. Catheter proximal motion data, which consists of 2 DoF axial (d) and rotational (θ) motions of the catheter were measured from the custom-designed sensors, as presented in previous works [9], through LabVIEW (National Instruments Corp., TX, USA) Recording of catheter tip positions and the proximal motion were synchronized and sampled at a rate of 33Hz. The experimental setups for data collection are shown in Fig. 3(a).

Catheter Motion Modeling: A training dataset from a demonstration is ($\lambda = \{t,x,y,z,d,\theta\}$), which consists of the time component, catheter tip position and axial/rotational motion signals. The datasets in each demonstration were manually segmented into three procedural phases: traversing the descending aorta, travel through the aortic arch and the cannulation of the innominate artery. Segmented datasets

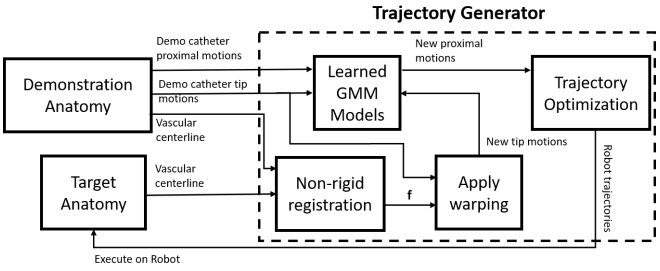

Fig. 2. A schematic diagram of the proposed robotic trajectory optimization method by incorporating anatomical information, 'Demo' is the short for "demonstration".

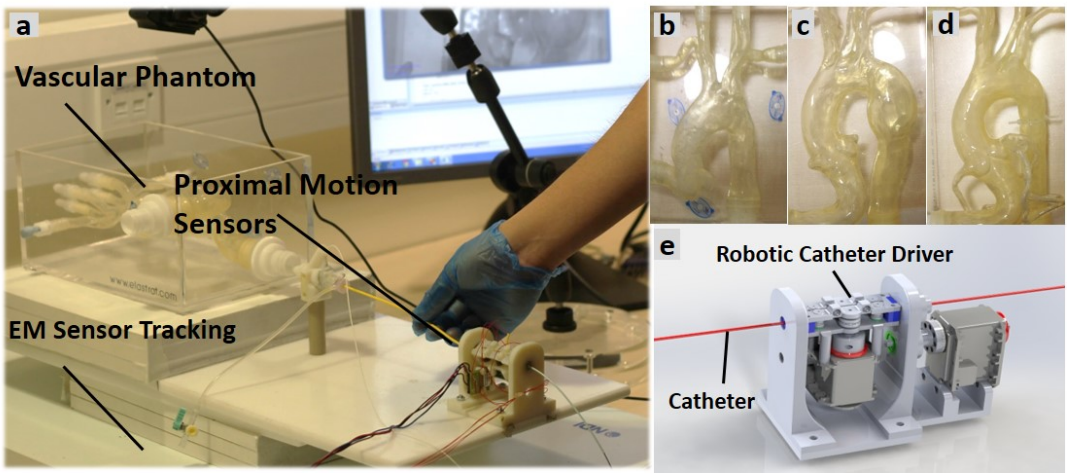

Fig. 3. (a) The experimental setup of data collection, (b) Vascular Phantom with a healthy arch, (c) Vascular phantom with aneurysm,(d) Vascular phantom with artificial stenosis, (e) CAD rendering of the robotic catheter driver.

from each phase were temporally aligned using Dynamic Time Warping (DTW). GMM was used to generate the probabilistic representation of the dataset. A GMM of K components can be defined as:

$$p(\lambda) = \sum_{k=1}^{K} p(k)p(\lambda|k) \tag{1}$$

The continuous observation probability distribution is $p(\lambda|k) = \mathcal{N}(\lambda|\mu_k, \Sigma_k)$ where μ_k and Σ_k are mean and covariance matrix of the Gaussian state k respectively. The GMMs were then trained by the Expectation Maximization (EM) algorithm for estimating the maximum log-likelihood of the GMM parameters. The optimal number of Gaussian components (K) were selected based on the Bayesian information criterion [13].

B. Catheter Tip Motion Transformation

The method of catheter tip motion transformation is based on the trajectory transfer algorithm previously reported in [7].The aim is to map the catheter tip trajectories from the demonstration anatomy into target anatomies. New tip trajectories were used to estimate new proximal motions of the catheter for the target anatomy. First, centerlines were extracted from 3D CT scans obtained from all three vascular phantoms by The Vascular Modeling Toolkit (vmtk), which represent the landmarks of the corresponding anatomy. The starting/ending positions of the centerlines extracted are the same as that of the demonstration task, hence the centerlines of all phantoms are anatomically equivalent. The non-rigid registration was performed between centerlines of the demonstration aorta and target anatomies, transformation function $\mathbf{f}$ was then used to warp the demonstrated tip trajectories into new anatomical situations. We used the Matlab libraires of Coherent Point Drift (CPD) algorithm [14] for non-rigd registration. For the centreline $\mathbf{X}$ in the demonstration anatomy that consists a of M $\times$ D matrix, where D is the dimension of the points. And centreline $\mathbf{Y}$ in the target anatomy with a N $\times$ D matrix. The result from the registration is to compute the warping function $\mathbf{f}$ that maps each point in $\mathbf{X}$ into the corresponding target point set $\mathbf{Y}$, which is equivalent to an optimization problem:

$$\underset{\mathbf{f}}{\textbf{minimize}} \left\{ -\sum_{n=1}^{N} log \sum_{m=1}^{M} e^{-\frac{1}{2}\left\|\frac{\mathbf{x}_n - \mathbf{y}_m}{\sigma}\right\|^2} \right\} + \text{REGULARIZER}(\mathbf{f}) \tag{2}$$

where the regularizer is a function that allow the transformation to be smooth. Then the transformation $\mathbf{f}$ was applied to warp the demonstrated trajectories.

In order to validate the accuracy of the transferred catheter tip trajectories after the registration. A cross validation was performed. The distance values calculated by DTW were used as a measure of similarity cost between the simulated tip motion trajectories with the demonstrated trajectories in the same vascular model. Firstly, the distance values were calculated between each two demonstrated trajectories in the same phantom, the largest distance value was set as the limit to assess on the transferred trajectories. Then each transferred trajectory was compare to all demonstrated trajectories, the transferred trajectory will be counted as accurate if the average distance value is smaller than the limit.

C. Trajectory Optimization and Robot Trajectory Generation

The learned GMMs were used to estimate the axial/rotational motions from the simulated catheter tip motions after the Non-rigid registration. The simulated tip positions ξ_t were used as query points to estimate the expected corresponding spatial distribution of axial/rotational motions ξ_p through the Gaussian Mixture Regression (GMR) [13]. The conditional probability of ξ_p regarding to ξ_t can be defined by:

$$\beta_k = \frac{p(\xi_t|k)}{\sum_{i=1}^{K} p(\xi_t|i)} \tag{3}$$

The obtained proximal motions were then smoothed by a further step of GMR to encode the essential features of the data into longer time steps. A new sequence of time-steps is used to estimate the corresponding spatial components of

the GMM. As a result, the smoothed axial/rotational motion trajectories were constructed from the training datasets in the demonstration phantom, to the other two target phantoms for the expert operator at each segmented phase of the task.

The optimized proximal motion trajectories were validated by a customized robotic catheter driver to perform cannulation to the innominate artery. The robotic driver is previously reported by the authors in [9](Fig. 3(e)) This driver consists of two servomotors which can push/pull and twist the catheter following the input trajectories. Catheter is driven by a pair of friction wheels that are directly coupled to one of the servomotors. The steering of the catheter is achieved by rotating the frame that holds the catheter. The robot is controlled by a PID controller. During the cannulation task, the robotic driver automates the catheter motion while an operator manipulates the guidewire for assistance. The maneuvers of the guidewire are 1) stationary in procedural phase one 2) insert through the aortic arch after phase one completes 3) retract after the phase two completes 4) insert when catheter tip is pointing to the innominate artery. The guidewire is carefully manipulated to avoid unwanted displacements of the catheter tip.

Catheter motions models from different experience levels were used to test the proposed framework. Demonstrations were collected from two novice operators (male, age of 24 and 27, engineering students) who have no prior knowledge or experience in endovascular tasks. The novice operators learned the procedures through watching the videos of expert's demonstrations, as well as practicing the tasks among the phantoms until repeatable skills were developed. Four demonstrations over each phantom were collected from each novice operator.

A cross validation was performed to find the success rate of cannulation to the innominate artery by the proposed framework. GMMs were generated from each phantom across each experience level. The demonstrated tip motions in each phantom were transferred into the other two phantoms. Robotic trajectories were estimated from each GMMs and optimized for target anatomies. The robotic driver was then used to execute the input trajectories and perform cannulation in the corresponding phantom. Successful cannulation will be counted if the final catheter tip position is within $\pm$ 2mm to the level of the destination position (bifurcation site in the innominate artery). 18 robotic cannulations were perform in the expert group and 36 cannulations in the novice group. (n = 3 for each phantom)

Catheterization Quality Evaluation: The quality of the proposed robotic approach is assessed. The catheter tip motions from the robotic approach were compared with demonstrated catheter tip motions by the expert operator. In this study, the demonstration anatomy is the healthy arch (Phantom A) whereas the target anatomies are diseased phantoms (Phantom B and C), which highlights the clinical importance of assessing on catheterization performance. Six robotic cannulations were performed in each phantom. The catheter tip positions were recorded by the EM position sensors. Tip kinematic metrics were calculated from the catheter tip trajectories. The metrics are: mean/maximum tip speed and acceleration, standard deviations of the speed, and total catheter path length (corresponding to the back and forth movements). All metrics over all phases were assessed using the non-parametric Wilcoxon rank-sum significance test (a value of $P<0.05$ was considered statistically significant). All data analysis were performed in Matlab. Based on those metrics, the performance of the robotic catheterization was compared with the actual demonstrated trajectories by the expert operator in the same vascular model.

The contact force sensing platform developed by the authors [15] was used in this paper to measure the contact forces exerted on the vasculature. Phantom A was mounted onto a plate that was fixed to a six-DoF force/torque (F/T) sensor (Mini40, ATI Industrial Automation, Inc., USA). Average root-mean-square (RMS) force modulus was calculated from the 3D forces measured from the F/T sensor, representing the interaction forces between the catheter and the vascular model. Two groups of proximal motion trajectories for Phantom A were estimated from demonstrations in Phantom B and C respectively. Those trajectories were then executed by the robot and the contact forces were recorded (n=6 for each group). The contact force data was then compared with that of manual catheterization from four expert operators performing the same cannulation tasks in the same vascular model (3 cannulations from each expert) . The expert contact force data was originally collected in previous works [15]. Metrics such as mean forces, maximum forces, standard deviations of the force and force impact over time were calculated from the force data in each cannulation. All metrics over all phases were assessed using the non-parametric Wilcoxon rank-sum significance test.

III. Experimental Results and Discussion

A. Catheter Motion Modeling

Fig. 4 shows the GMMs of both axial/rotational motion trajectories and catheter tip motion trajectories in the phase of descending aorta. The colored ellipsoids represent the GMM components, where the same color represents the same GMM component.

B. Catheter Motion Transformation

For the validation the catheter motion transformation, 36 simulated tip trajectories were generated from the expert group (12 from each phantom). 48 simulated tip trajectories were generated from the novice group (8 from each phantom). 86.1%(31/36) of the trajectories in the expert group were classified as accurate. 91.6%(44/48) trajectories from the novice dataset were classified as accurate. Results show that the majority of the demonstrated trajectories can be mapped to different anatomical settings.

C. Experiments with the Robotic Platform

The cross validations for the proposed robotic platform were performed to test the simulated robotic trajectories on different vascular phantoms. For the expert dataset, 100% (18/18) of the cannulation tasks succeed. 94.4% (34/36) of

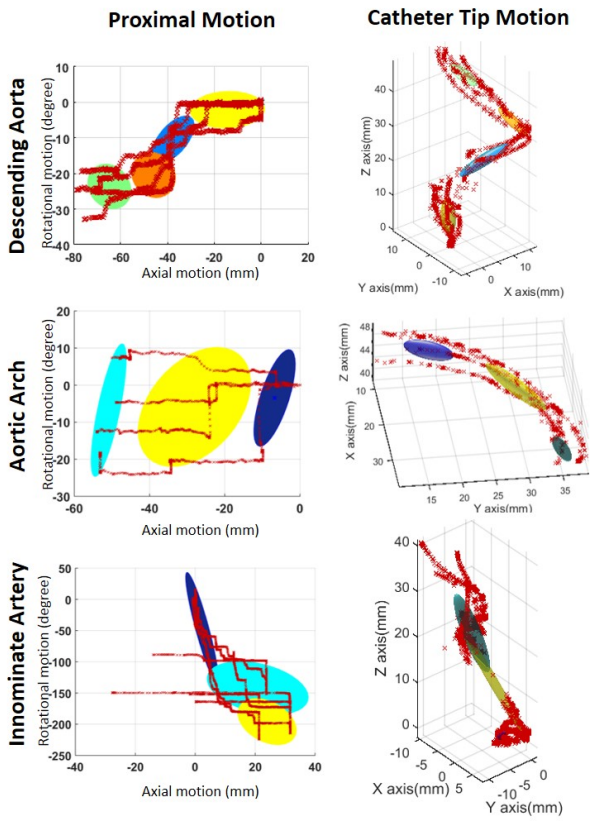

Fig. 4. Training data from the demonstrations (red lines) and learned GMMs (colored ellipsoids) of catheter proximal motion (left) and tip motion (right)

TABLE I

MEDIAN VALUES FOR STATISTICALLY SIGNIFICANT DIFFERENCES (P <0.05) BETWEEN ROBOT-ASSISTED LEARNED PROCEDURES VS. CORRESPONDING EXPERT MANUAL DEMONSTRATING DATA WITHIN DIFFERENT ANATOMIES.

	Aneurysm Model		Stenosis Model	
Expert	Manual	Robot	Manual	Robot
mean speed (mm/s)	6.75	2.78	4.16	2.17
max speed (mm/s)	356.3	124.7	255.0	177.5
STDEV speed (mm/s)	20.7	4.56	23.4	7.01
mean acceleration (mm/s^2)	226.1	104.8	139.2	77.4
max acceleration (mm/s^2)	1.15×10^5	2.80×10^4	8.02×10^4	5.27×10^4
path length (mm)	360.5	281.2	-	-

the tasks were completed for the novice dataset. All experiments successfully finish the cannulation to the innominate artery. For the failed case in the novice group, the robot failed to reach the destination position in the last phase. This was due to buckling of the catheter in the descending aorta. The high success rates suggest that the proposed framework is able to adapt to anatomical variability across structurally similar vessels. This method is also applicable to operators within different experience levels.

Table. I shows the result of the non-parametric test, with median values for statistically significant differences (P <0.05) between the manual approach and the proposed

TABLE II

MEDIAN VALUES FOR STATISTICALLY SIGNIFICANT DIFFERENCES (P <0.05) BETWEEN CONTACT FORCES EXERTED ON THE VASCULATURE FROM ROBOT-ASSISTED PROCEDURES VS. EXPERT MANUAL PROCEDURE IN PHANTOM A

	Manual	Robotic
mean force (N)	0.225	0.150
maximum force (N)	1.29	0.555
STDEV force (N)	0.309	0.0907
force impact area (N.s)	8.09	16.0

robotic approach. Compare to manual catheterization. It is evident that for robotic driver performed a slower catheterization in the two target phantoms at lower speed and acceleration. In both case, the standard deviations of the speed are significantly lower, which suggest more continuous and controlled catheter motions. The robotic approaches in Phantom B, can achieve a shorter path length compare to the manual approach , suggests reduced overall back and forth movements of the catheter tip, potentially leads to less vessel wall contacts and hence reduces risks associate with dissection, perforation, thrombosis and stroke in the clinical situation. which is particularly important in the presence of diseased vessels (such as Phantom B and C).

Fig. 5 depicts examples of the catheter paths and tip displacements of the robotic approaches and manual approaches across different phantoms. Robotic Trajectories were estimated from the demonstrations in Phantom A and were executed in Phantom B and C. Comparing tip displacements obtained by the robotic driver to that of the manual catheterization, in both case, the catheter driven by the robot achieved more continuous and smoother tip displacements. The manual approaches in contrast, achieved steeper displacements in the first procedural phase and overall faster than the robot.

Fig. 6 shows an example of the differences between manual and robotic approaches using the forces measured over time, this graph highlights the lower force values seen during robotic manipulation. Compare to the expert operator, the robotic approach takes longer than the manual approach; however, there is less perturbation of forces over time and significantly lower forces were observed in some parts of the procedure. The metrics shown in Table II provide more insights into the forces applied to the vasculature. Both mean forces and maximum forces are significantly lower during the robotic catheterization than that of the manual techniques. The standard deviations of the forces is significantly lower in the robotic approach, which suggests more continuous, stable and repeatable catheter motions. However, the force impact over time is significantly higher in the case of robotic manipulation since the procedure takes longer.

IV. CONCLUSION AND FUTURE WORK

This paper proposes an improved robotic platform for semi-automatic endovascular catheterization, through using non-rigid registration to find warping function between anatomical landmarks that allows to map demonstrated

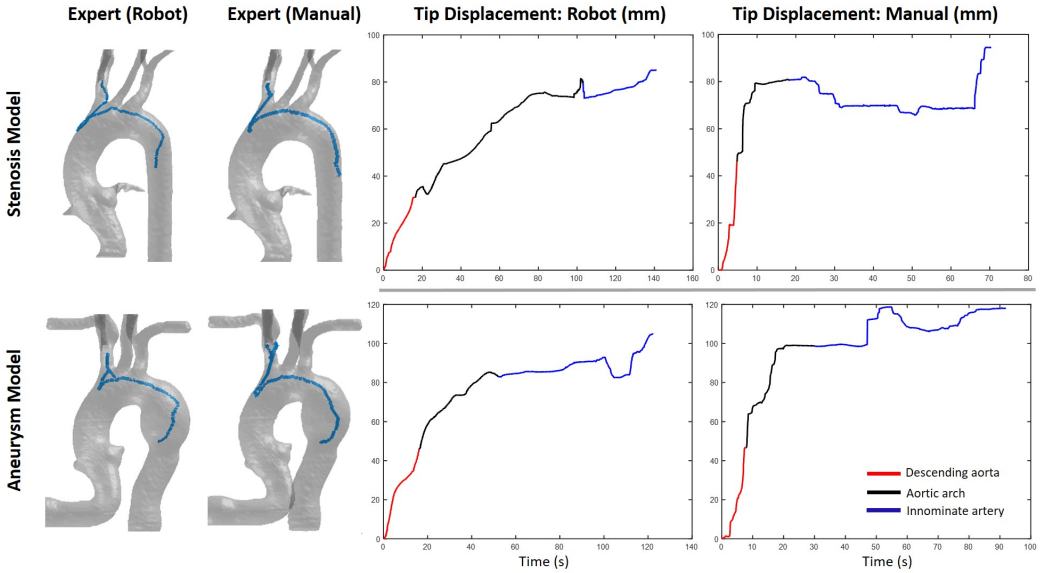

Fig. 5. Catheter path and tip displacement obtained by robotic approach vs. the manual approach within different models. Different colors represent segmented phases of the task.

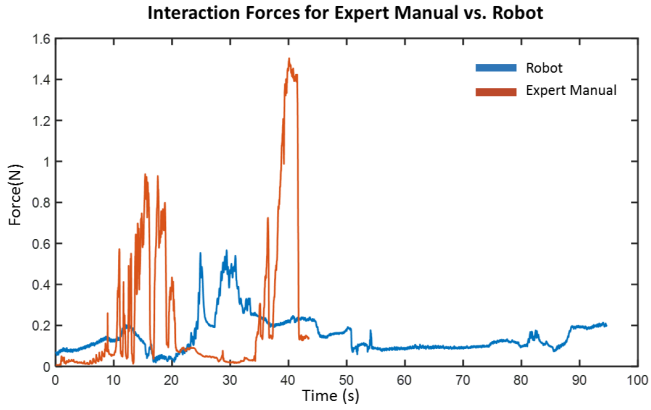

Fig. 6. An example of contact forces exerted by expert (orange color) operator and the robot (blue color) for cannulation of innominate artery in Phantom A.

catheter tip trajectories into different anatomical settings. Underlying motion patterns from catheter proximal motions and tip motions were extracted and encoded by statistical modeling. Transferred tip trajectories and the learned models were used as a trajectory generator to optimize trajectories for subject-specific anatomies. Experiments shows high success rate of a cannulation task by using the proposed trajectory generator and the robotic catheter driver onto different aortic arch models. The quality of the robotic catheterization was assessed through comparing tip kinematics to that of the manual approach. Smoother, more continuous and shorter path length were observed from the results, which indicate safer and more controlled catheter motions. Moreover, the proposed robotic approach is compared to the manual techniques by measuring contact forces exerted by the catheter to the vasculature, the robot achieved significantly reduced mean and maximum forces than the manual approaches over time, and significantly smoother force patterns. Future improvements of the robotic platform include adding dynamic flow simulation into the vascular phantoms and improved realism, incorporating dynamic shape modeling with real-time trajectories optimization. The learning of catheter tip motion and proximal motion also provide insights into modeling control policies of standard catheters. The methods proposed in this paper can be used for modeling skills associated with other endovascular instruments, more complex endovascular procedures and navigation for more angulated vasculatures.

REFERENCES

[1] C. V. Riga, C. D. Bicknell, A. Rolls, N. J. Cheshire, and M. S. Hamady, "Robot-assisted fenestrated endovascular aneurysm repair (FEVAR) using the Magellan system," J Vasc Interv Radiol, vol. 24, pp. 191-6, Feb 2013.

[2] H. Rafii-Tari, C. J. Payne, and G.-Z. Yang, "Current and Emerging Robot-Assisted Endovascular Catheterization Technologies: A Review," Annals of Biomedical Engineering, vol. 42, pp. 697-715, 2014.

[3] Y. Thakur, D. W. Holdsworth and M. Drangova, "Characterization of Catheter Dynamics During Percutaneous Transluminal Catheter Procedures," in IEEE Transactions on Biomedical Engineering, vol. 56, no. 8, pp. 2140-2143, Aug. 2009. Eng. 56(8), 21402143 (2009)

[4] B. D. Argall, S. Chernova, M. Veloso, and B. Browning, "A survey of robot learning from demonstration," Robotics and Autonomous Systems, vol. 57, pp. 469-483, 5/31/ 2009.

[5] J. van den Berg et al., "Superhuman performance of surgical tasks by robots using iterative learning from human-guided demonstrations," 2010 IEEE International Conference on Robotics and Automation, Anchorage, AK, 2010, pp. 2074-2081.

[6] N. Padoy and G. D. Hager, "Human-Machine Collaborative surgery using learned models," 2011 IEEE International Conference on Robotics and Automation, Shanghai, 2011, pp. 5285-5292.

[7] J. Schulman, J. Ho, C. Lee, and P. Abbeel, "Learning from Demonstrations Through the Use of Non-rigid Registration," in Robotics Research: The 16th International Symposium ISRR, M. Inaba and P. Corke, Eds., ed Cham: Springer International Publishing, 2016, pp. 339-354.

[8] T. Osa, N. Sugita, and M. Mamoru, Online Trajectory Planning in Dynamic Environments for Surgical Task Automation, in Robotics: Science and Systems (RSS), 2014.

[9] H. Rafii-Tari, J. Liu, S.-L. Lee, C. Bicknell, and G.-Z. Yang, "Learning-Based Modeling of Endovascular Navigation for Collaborative Robotic Catheterization," in Medical Image Computing and Computer-Assisted Intervention MICCAI 2013: 16th International Conference, Nagoya, Japan, September 22-26, 2013, Proceedings, Part II, K. Mori, I. Sakuma, Y. Sato, C. Barillot, and N. Navab, Eds., ed Berlin, Heidelberg: Springer Berlin Heidelberg, 2013, pp. 369-377.

[10] V. Y. Reddy, P. Neuzil, Z. J. Malchano, R. Vijaykumar, R. Cury, S. Abbara, et al., "View-Synchronized Robotic Image-Guided Therapy for Atrial Fibrillation Ablation," Experimental Validation and Clinical Feasibility, vol. 115, pp. 2705-2714, 2007.

[11] I. Cheng, A. Firouzmanesh, A. Lelev, R. Shen, R. Moreau, V. Brizzi, et al., "Enhanced Segmentation and Skeletonization for Endovascular Surgical Planning," in SPIE 2012, San Diego, United States, 2012, p. 83162W.

[12] H. Rafii-Tari, J. Liu, C. J. Payne, C. Bicknell, and G.-Z. Yang, "Hierarchical HMM Based Learning of Navigation Primitives for Cooperative Robotic Endovascular Catheterization," in Medical Image Computing and Computer-Assisted Intervention, 2014, pp. 496-503.

[13] S. Calinon, F. Guenter and A. Billard, "On Learning, Representing, and Generalizing a Task in a Humanoid Robot," in IEEE Transactions on Systems, Man, and Cybernetics, Part B (Cybernetics), vol. 37, no. 2, pp. 286-298, April 2007.

[14] A. Myronenko and X. Song, "Point Set Registration: Coherent Point Drift," in IEEE Transactions on Pattern Analysis and Machine Intelligence, vol. 32, no. 12, pp. 2262-2275, Dec. 2010.

[15] H. Rafii-Tari, C. J. Payne, J. Liu, C. Riga, C. Bicknell and G. Z. Yang, "Towards automated surgical skill evaluation of endovascular catheterization tasks based on force and motion signatures," 2015 IEEE International Conference on Robotics and Automation (ICRA), Seattle, WA, 2015, pp. 1789-1794.